ISSN (Print) 1226-1750
ISSN (Online) 2233-6656
Journal of Magnetics 23(1), 74-78 (2018) https://doi.org/10.4283/JMAG.2018.23.1.074

Experimental and Analytical Study of Surface-Mounted Type Variable Flux Permanent Magnet Motor Considering Controllable Magnet Properties

Kyu-Seok Lee[1,2], Sung-Ho Lee[1]*, Jung-Hyung Park[1], and Jang-Young Choi[2]

[1]*Seonam Regional Division, Korea Institute of Industrial Technology, Gwangju 61012, Republic of Korea*
[2]*Department of Electrical Engineering, Chungnam National Univerisity, Daejeon 34134, Republic of Korea*

(Received 1 September 2017, Received in final form 27 December 2017, Accepted 28 December 2017)

A variable flux permanent magnet motor (VFPMM) alters its characteristics at low and high-speeds by changing the magnetic flux of a variable magnet. In this paper, a motor capable of varying its magnetic flux based on the slot/pole structure is proposed. In addition, the variation characteristics of flux density and field intensity of a variable magnet in the VFPMM under magnetization/demagnetization conditions are analyzed using the finite element method (FEM) and experimentation. A prototype was tested for the magnetization/demagnetization characteristics, and it was confirmed that the value of the measured back EMF was nearly identical to the corresponding values obtained by an FEM analysis. Finally, the characteristics of the VFPMM for each magnetization/demagnetization state were evaluated at both low- and high-speed ranges. To verify the effect of variable flux, experimental results are also presented.

Keywords : variable flux, permanent magnet motor, magnetization and demagnetization, control magnet property

1. Introduction

PERMANENT MAGNET (PM) MACHINES have been used for electric vehicles and home appliances because of their high-efficiency, high-torque and compact size. A PM motor has a higher efficiency than currently available induction motors because the permanent magnet serves as the magnetic field, thereby preventing any loss in the rotor. On the other hand, a PM motor has the disadvantage of its inability to ensure high driving speeds during variable speed driving because the magnetic flux of the permanent magnet cannot be controlled. Thus, for the case of PM motors, demagnetization current is provided during high-speed driving so that the magnetic flux is reduced.

As such, PM motors have drawbacks including a high d-axis current and reduced efficiency due to the flux-weakening control used during high-speed operation [1-3]. For example, a PM in a washing machine has a wide driving range from low speed during washing cycle to high speed during drying. Therefore, it has a comparatively wider speed range than that of motors in other home appliances.

©The Korean Magnetics Society. All rights reserved.
*Corresponding author: Tel: +82-62-6006-350
Fax: +82-62-6006-219, e-mail: shlee07@kitech.re.kr

A flux-weakening control, which reduces its efficiency during high-speed operations, is needed. For this reason, it is difficult to achieve high efficiency with a broad range of speeds when using PM motors. To solve this problem, a motor with the ability to control the magnetization/demagnetization levels according to the drive speed, i.e., a variable flux permanent magnet motor (VFPMM), was proposed [4, 5].

A variable flux motor with high efficiency at low speeds was studied for driving a sufficient magnetization of the magnet to generate high-torque. This motor facilitated high efficiency drive by reducing the current capacity required to control a weak field by demagnetizing the magnet at high speeds.

In this paper, a surface-mounted type VFPMM is designed using the previously mentioned properties. First, the concept of an SPM-Type VFPMM is proposed through which any magnetization/demagnetization structure can be obtained by varying the combination of slots/poles and variable magnet arrangement.

The magnetization/demagnetization characteristics of the variable magnet in the suggested structure are then verified by comparing the finite element method (FEM) results using the hysteresis curve of the controlled magnet properties. A prototype was manufactured to test the variable characteristics of each magnetization/demagneti-

© 2018 Journal of Magnetics

zation current and the motor load.

2. Machine Structure and Design

2.1. Structure of magnetization/demagnetization

A VFPMM was proposed in the early 2000s. This motor had a rotor manufactured as a type of magnet [4]. If the magnetization/demagnetization current is applied in one phase, which serves as a reference axis, to magnetize/demagnetize the variable magnet that constitutes the rotor, the magnitude of the back EMF waveform for each phase remains identical.

The VFPMM suggested in this paper, however, uses two different types of magnets. Thus, the arrangement and combination of the slot/pole pairs around each magnet is analyzed, and the magnitude of the measured back EMF for each phase is designed to be identical. The two types of magnets used have different attributes such as Br values and weight. Thus, the motor should be designed considering of the weight distribution cross the entire structure of the rotor, so that noise and vibration resulting from any magnetic field imbalance are minimal.

Fig. 1 shows the 36 slot 48 pole structure of VFPMM, which has 6 variable magnets that generate the same magnitude of back EMF waveform after the magnetization/demagnetization current is supplied. In Fig. 1(a) and (b), the position of the variable magnet is different, but the number of variable magnets is 6, so that the same variable effect can be obtained.

To obtain a variable magnetic flux of the same condition, the following condition is required.

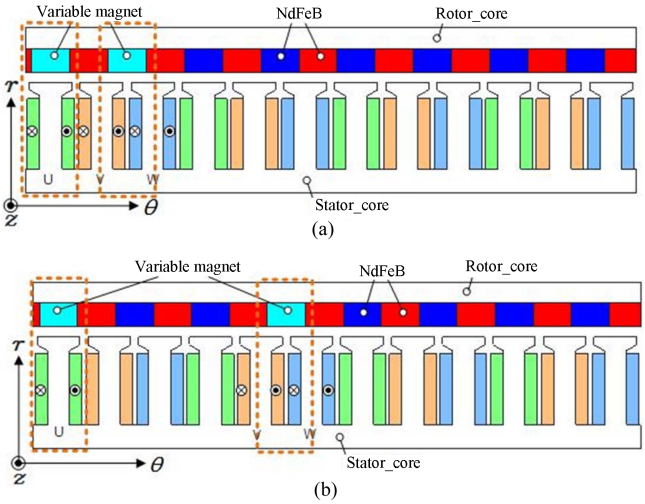

Fig. 1. (Color online) Magnet arrangement with 6 variable magnets (1/3 segment structure). (a) Arrangement type 1 with 6 variable magnets, (b) Arrangement type 2 with 6 variable magnets.

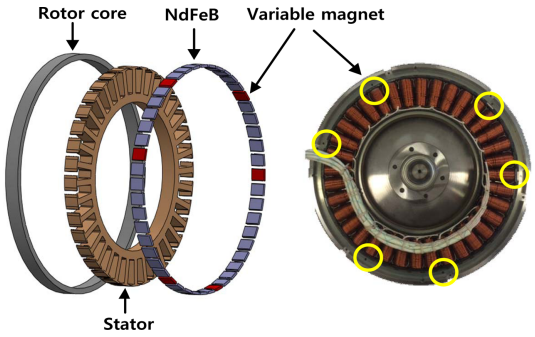

Fig. 2. (Color online) Configurations of the proposed SPM VFPMM.

$$N_{spp} = \frac{N_s}{N_m N_{ph}} = 0.25(N_{ph} = 3) \quad (1)$$

- U_{ph} is vertically aligned with the variable magnet (d-axis alignment), when the other variable-flux magnets d-axis is aligned between the V_{ph} and W_{ph}.
- Stator winding pattern is a concentrated winding.
- Number of Variable magnets is $2 \times n\left(n \le \frac{N_m}{4}\right)$

Where N_{spp} is number of slots per pole per phase, N_s is number of slots, N_m is number of magnet poles, N_{ph} is number of phases. The number of slots/poles that can be obtained in the VFPMM structure according to these conditions are 3/4, 9/12, 12/16, 15/20, 18/24, 21/28, 36/48, and so on.

2.2. Structure of Proposed VFPMM

The magnetization/demagnetization structure and the VFPMM design are shown in Fig. 2. The rotor structure of the VFPMM consists of 36 slots and 48 poles. For the magnet, a Alnico magnet with a variable flux that can replace 6 of the 48 poles that were designated as the surface-mounted type; NdFeB was used for the rest of the magnets.

The main specifications of the VFPMM are given in Table 1.

3. Magnetization/Demagnetization Method

The electric circuit for magnetization/demagnetization is shown in Fig. 3. The VFPMM has the ability to change

Table 1. Dimensions and parameters of a VFPMM.

Parameter	Value	Parameter	Value
Slots and poles	36/48	Stack	20 mm
Stator outer diameter	259 mm	NdFeB Magnet	38sh
Stator inner diameter	158 mm	Variable Magnet	Alnico
Rotor Outer diameter	281 mm	Turns	98

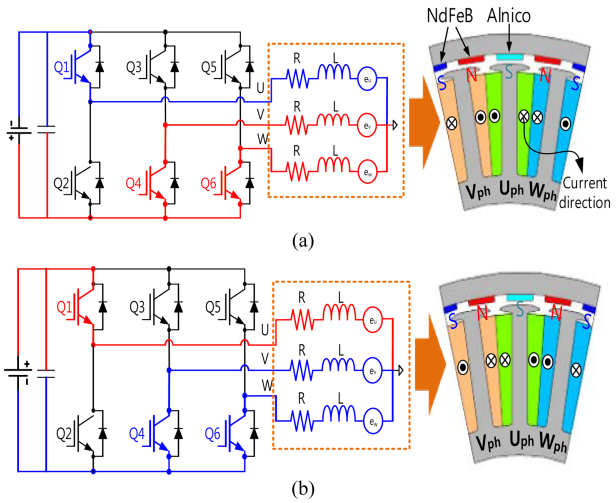

Fig. 3. (Color online) Electric circuit of magnetization/demagnetization. (a) Magnetization circuit, (b) Demagnetization circuit.

the intensity of the magnetization/demagnetization using a short current pulse through the stator windings for a very short period of time inside the Alnico magnets [6].

3.1. Method of FEM Analysis

To verify the magnitude of the magnetization/demagnetization currents for magnetizing/demagnetizing the Alnico magnet, an FEM analysis was conducted. The magnetic field distribution inside the Alnico magnet was analyzed using the magnetization/demagnetization current.

Fig. 4 and 5 show the flux distributions and magnetic fields inside the Alnico magnet when a magnetization current and demagnetization current of 15 A and 10 A, respectively, are applied. Br value can be derived from the hysteresis curve of the Alnico magnet based on the magnetic field values obtained by the FEM analysis.

3.2. Analysis of PM Hysteresis

Fig. 6 shows the hysteresis curve of the Alnico magnet. The magnet operating point in the hysteresis curve is

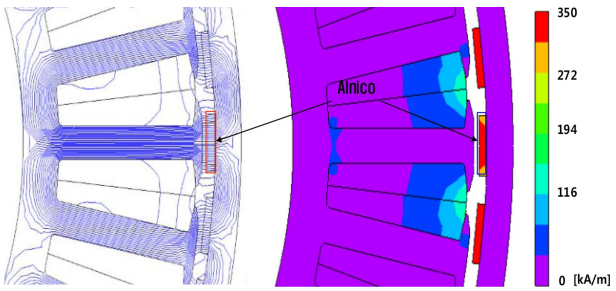

Fig. 4. (Color online) Flux and magnetic field distribution in Alnico magnet under 15 A magnetization current.

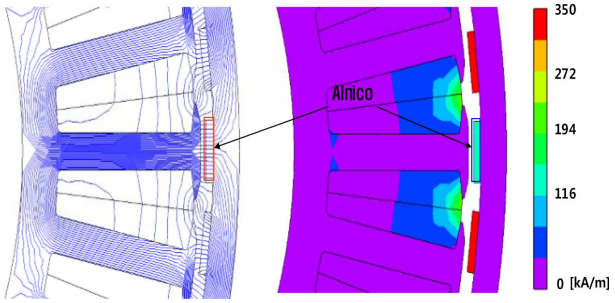

Fig. 5. (Color online) Flux and magnetic field distribution in Alnico magnet under 10 A demagnetization current.

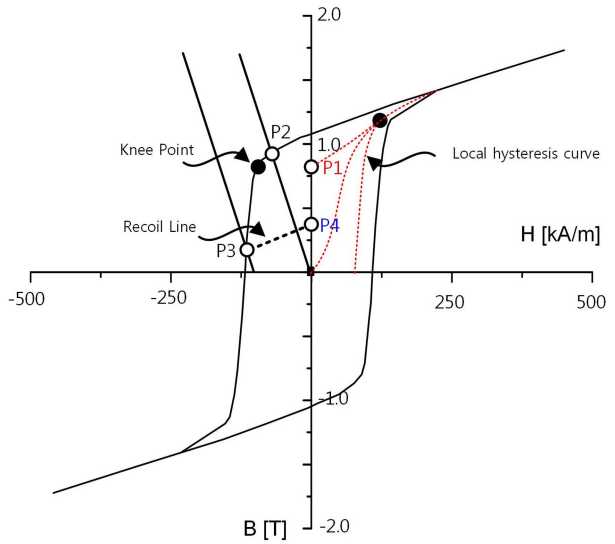

Fig. 6. (Color online) Hysteresis curve for the Alnico magnet.

inferred with the magnetic field value inside the Alnico magnet by the magnetization current. A P1 value can be calculated from the local hysteresis curve for each magnetization condition. The local hysteresis curve was created on the basis that the saturation point was calculated using an FEM analysis, and it can be used to estimate the P1 point under magnetization. The magnitude of back EMF is reanalyzed by FEM using the B_H curve at the P1 point [6, 7].

The magnetic field inside the Alnico magnet using an FEM analysis was 310-325 kA/m, when the magnetization current was 15 A. The remanence on the first quadrant magnetization curves with the above magnetic field value is identical to a fully magnetized state.

In contrast to the magnetization properties, a demagnetizing field was applied to make the magnet operating point move from P2 to P3 below the knee point, the operating point will return along another recoil line P3-P4 due to the irreversible demagnetization [7]. Therefore, the magnetic field produced by the demagnetization current can

be calculated by the P4 value below the knee point. The FEM analysis using the B_H curve for the P4 point was conducted. The magnetic field inside of the Alnico magnet by FEM analysis was −121 ~ −144 kA/m, when the demagnetization current was 10 A. The remanence on the recoil line with the above magnetic field value is identical to a fully demagnetized state.

4. Experimental Verification

4.1. Test of magnetization/demagnetization

To verify the results from the FEM analysis of the magnetization/demagnetization condition, the back EMF after applying magnetization/demagnetization current to a prototype was evaluated.

The FEM and measured back EMF waveforms of phase at 50 rpm under a 10 A demagnetization are shown in Fig. 7. The results for a 10 A demagnetization condition

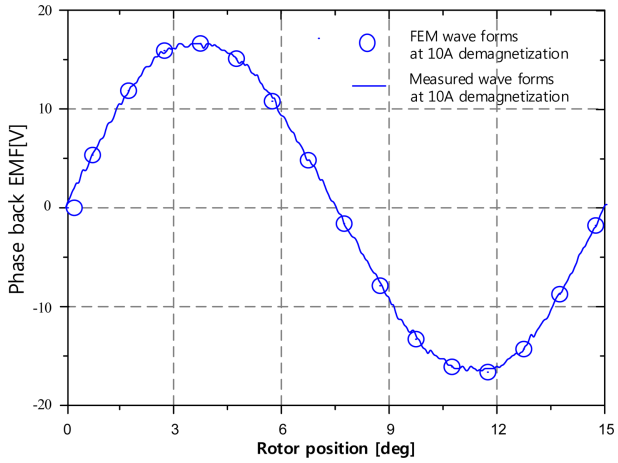

Fig. 7. (Color online) Measured and FEM results for the phase back EMF waveforms under 10A-Demagnetization.

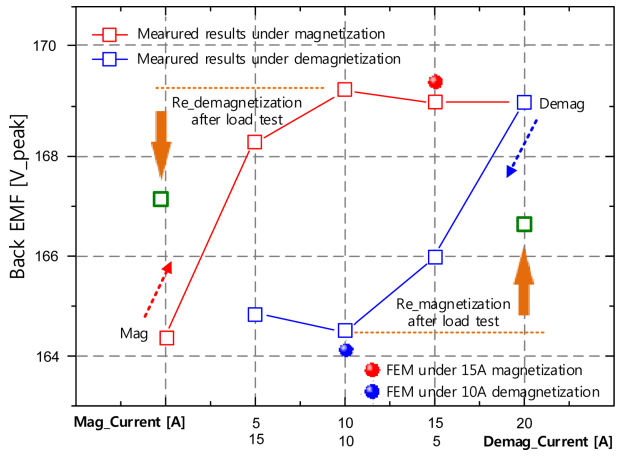

Fig. 8. (Color online) Experimental and FEM results at 500 rpm for each magnetization/demagnetization condition.

was confirmed, and the waveform from the FEM analysis is nearly identical to the experiment results. The measured phase back EMF peak values at 500 rpm under each magnetization/demagnetization condition are shown in Fig. 8. It confirms that the FEM analysis and experimental results based on the magnetization/demagnetization current were nearly identical. The variable amounts of back EMF at a 500 rpm were confirmed to be 4.5 V when 6 Alnico magnets for variable flux were used.

By obtaining the internal magnetic field changes using magnetization/demagnetization currents and further determining the P1 and P4 values on the Alnico hysteresis curve, the magnetization/demagnetization characteristics of VFPMM were verified by FEM analysis and experimental testing results.

4.2. Load test for VFPMM

Fig. 9 shows the load test set of the fabricated VFPMM with 6 variable magnets. The load evaluation after applying a full magnetization current (15 A) into the Alnico magnets of the prototype was conducted from 50-1250 rpm. Also, the load test after a applying full demagnetization current (10 A) into the Alnico magnets was conducted. Fig. 10(a) and (b) show the load experimental results in low and high-speed ranges.

The constant torque control and the constant output control of the controller were performed to drive the VFPMM. The constant torque control is performed up to 50-300 rpm based on the maximum torque of 23 Nm of the VFPMM.

In the speed range greater than 300 rpm, which is the flux-weakening control, constant output control was performed based on the output 500 W.

At a washing operation condition of 50 rpm, the efficiency of the VFPMM after magnetization was 66.73 %, which was about 0.54 % higher than that of the washing

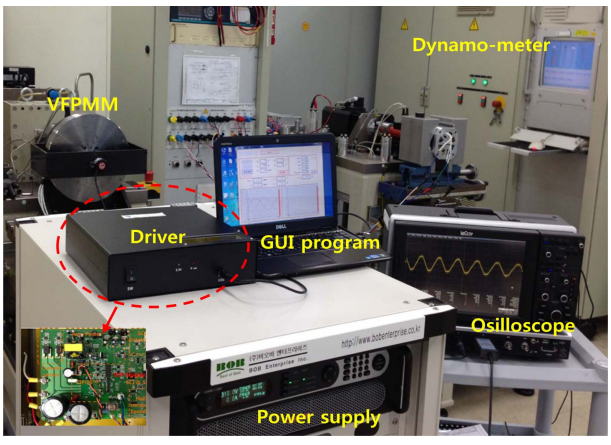

Fig. 9. (Color online) Load experimental test.

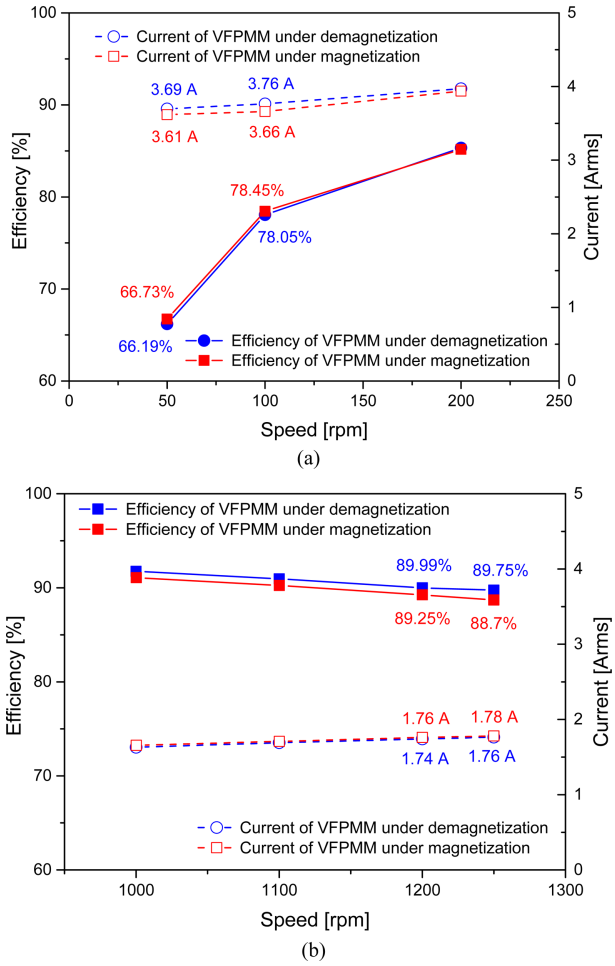

Fig. 10. (Color online) Load experimental results for VFPMM under magnetization and demagnetization. (a) Low speed (50-200 rpm) (b) High speed (1000-1250 rpm)

mode after demagnetization.

Also, it was confirmed that the efficiency of VFPMM after demagnetization was 89.75 % at 1250 rpm, and about 1.05 % higher than the efficiency after magnetization.

However, as shown in Fig. 8, the magnitude of the back EMF by load current is decreased after the load test, when the VFPMM is magnetized. The magnitude of the back EMF by load current increased after the load test, when the VFPMM is demagnetized. In other words, the amount of variable magnetic flux at load test was confirmed to be reduced from 4.5 V to 0.5 V at 500 rpm.

5. Conclusion

The proposed VFPMM adjusts its performance during low- and high-speed ranges by altering the magnetic flux from the Alnico magnets. In this paper, the structure of the VFPMM was analyzed. The magnetization/demagnetization characteristics of the VFPMM can be predicted using FEM analysis and hysteresis curves. The FEM results matched well with the experimental results from a fabricated prototype. Furthermore, a load evaluation was performed for all magnetization-/demagnetization conditions.

In the low speed range, the efficiency of the VFPMM in magnetized state was higher than that of the VFPMM in the demagnetized state.

On the contrary, in the high speed range, the efficiency of the VFPMM in the demagnetized state was higher than that of VPFMM in the magnetized state.

Based on the these results, it is confirmed that the performance of the motor could be adjusted by altering the magnetic flux of the motor depending on the range of drive speeds required, which is the characteristic of a VFPMM.

References

[1] T. Jahns, IEEE Trans. Ind. Appl. **IA-23**, 4 (1987).
[2] Kazuto Sakai, Kazuaki Yuki, Yutaka Hashiba, Norio Takahashi, and Kazuya Yasui, Electrical Machines and Systems, (2009).
[3] Y. Liu, J. Zhao, and R. Wang, IEEE Trans. Power Electron. **28**, 5 (2013).
[4] V. Ostovic, IEEE Trans. Ind. Appl. **39**, 1 (2003).
[5] Sari Maekawa, Kazuaki Yuki, Makoto Matsushita, Isamu Nitta, Yukihisa Hasegawa, Tsuyoshi Shiga, Tsuyoshi Hosoito, Kazunobu Nagai, and Hisao Kubota, IEEE Trans. Power Electron. **29**, 9 (2014).
[6] Hengchuan Liu, Heyun Lin, Shuhua Fang, and Z. Q. Zhu, IEEE Trans. Magn. **45**, 10 (2009).
[7] Hengchuan Liu, Heyun Lin, Z. Q. Zhu, Mingming Huang, and Ping Jin, IEEE Trans. Magn. **46**, 6 (2010).
[8] H. C. Lovatt and P. A. Watterson, IEEE Trans. Magn. **35**, 1 (1999).